NANO LETTERS

Letter

Direct Observation of the Radial Breathing Mode in CdSe Nanorods

Holger Lange, Marcel Mohr, Mikhail Artemyev, Ulrike Woggon, and Christian Thomsen

Nano Lett., **2008**, 8 (12), 4614-4617 • DOI: 10.1021/nl803134t • Publication Date (Web): 05 November 2008

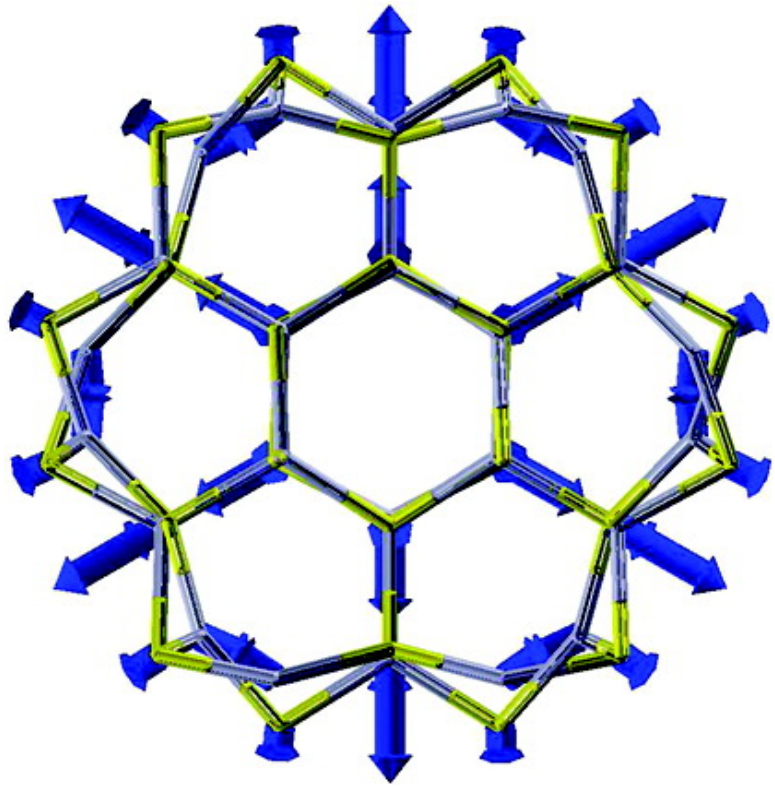

NANO LETTERS

2008
Vol. 8, No. 12
4614-4617

Direct Observation of the Radial Breathing Mode in CdSe Nanorods

Holger Lange,*,† Marcel Mohr,† Mikhail Artemyev,‡ Ulrike Woggon,§ and Christian Thomsen†

Institut für Festkörperphysik, Technische Universität Berlin, Germany, Institute for Physico-Chemical Problems of Belorussian State University, Minsk, Belarus, and Institut für Optik und Atomare Physik, Technische Universität Berlin, Germany

Received October 16, 2008

ABSTRACT

We experimentally confirm the existence of the radial breathing mode in CdSe nanorods by Raman spectroscopy, which was deduced from ab initio calculations of the vibrational properties of bare CdSe nanowires and CdSe/ZnS core−shell nanowires. We calculated the modes' frequency for various diameters and measured a set of bare CdSe nanorods and CdSe/ZnS core−shell nanorods to determine the diameter dependence of the modes' frequency. The frequency of this mode is strongly diameter dependent and it can be used to estimate the nanorod diameter from a Raman measurement alone.

Direct band gap semiconductor nanocrystals possess size-dependent optical and electronic properties and thus offer a huge potential for applications in the field of optoelectronics and biotechnology. Advanced growth techniques allow the synthesis of semiconductor nanocrystals into rod-shaped structures with defined sizes and narrow size distributions.[1] The control of the growth kinetics of the II−IV semiconductor CdSe, for example, results in nanostructures of various shapes, from spherical nanospheres to nanorods with well-defined diameters and aspect ratios.[2] CdSe nanorods with narrow size distributions, diameters of 3 nm and aspect ratios up to 20:1 can be achieved in large scales[3] and even smaller structures with diameters below 2 nm and an aspect ratio of 5:1 have been reported.[4] The nanorods demonstrate a size-dependent photoluminescence that covers the visible spectrum.[5] The possibility to coat the CdSe nanorods with an epitaxial shell of a larger-bandgap material, like ZnS, is an important enhancement for applications. The ZnS shell increases the luminescence efficiency, decreases the laser threshold, and gives rise to further surface modifications that allow, e.g., biocompatibility.[3,6] Thus, they are interesting for both fundamental research[7−9] and technological applications.[10,11] The characterization of such small structures, however, requires sophisticated methods like high-resolution transmission electron microscopy.

In another well-studied low-dimensional structure, the carbon nanotubes (CNTs), details about the exact geometry can be easily obtained by purely optical measurements. The radial breathing mode (RBM) in CNTs corresponds to the atomic vibration of the carbon atoms in the radial direction, as if the tube was breathing, and its frequency is highly diameter sensitive. Resonant Raman measurement of the RBM in CNTs is a standard, straightforward method to precisely determine the CNT diameter and characterize CNT conglomerates.[12−14] Our calculations of the vibrational properties of several different-sized CdSe nanowires (NWs) reveal the presence of a similar, fully symmetric, and diameter-sensitive vibrational mode in the NWs.

In this Letter we present the first direct experimental observation of the RBM in nanorods. We used Raman scattering experiments on a set of colloidal CdSe nanorods, partly with ZnS shell, and ab initio calculations of the vibrational properties of bare CdSe NWs, CdSe/ZnS core−shell NWs to estimate the diameter dependence of the modes' frequency and to observe changes of the RBM with addition of a ZnS shell.

Results and Discussion. The RBM of a NW is similar to the RBM of a CNT but for a solid cylinder instead of a tube. The frequency dependence of such a mode can be estimated from linear elasticity theory. For a long isotropic cylinder the frequency of such a mode is given by[15]

$$\omega = \frac{2\tau_n}{d}\sqrt{\frac{E(1-\nu)}{\rho(1+\nu)(1-2\nu)}} \qquad (1)$$

where ν is Poisson's ratio and ρ and E are the density and Young's modulus of the nanorod material. τ_n is the nth root of the equation $\tau J_0(\tau) = [(1-2\nu)/(1-\nu)]J_1(\tau)$, where J_m values are the Bessel functions of the first kind. The square root in eq 1 depends only on the material properties; the

* Corresponding author, holger.lange@physik.tu-berlin.de.
† Institut für Festkörperphysik, Technische Universität Berlin.
‡ Institute for Physico-Chemical Problems of Belorussian State University.
§ Institut für Optik and Atomare Physik, Technische Universität Berlin.

10.1021/nl803134t CCC: $40.75
Published on Web 11/05/2008

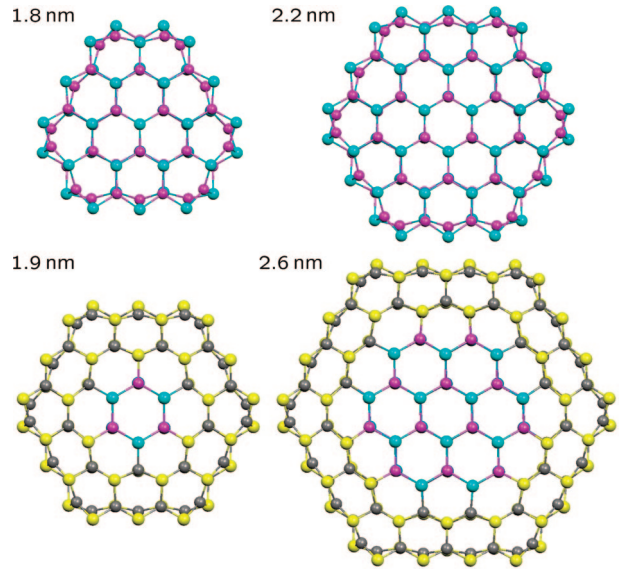

Figure 1. Cross sections of come of the calculated CdSe nanowires. The individual profiles are labeled by their diameter. The following color code is used: Cd (magenta), Se (cyan), Zn (black), S (yellow).

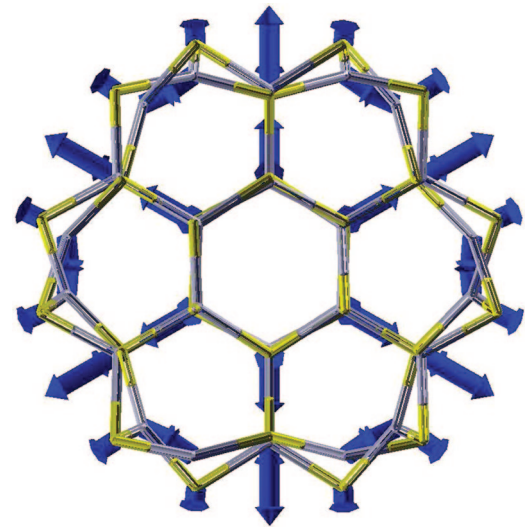

Figure 2. Calculated displacement pattern of the breathing mode of a 1.4 nm diameter CdSe nanowire.

diameter dependence of this radial modes' frequency is thus proportional to $1/d$. The same diameter dependence has also been deduced from a Stillinger−Weber-type model for calculated Raman spectra of Si[111] nanowires by Thonhauser and Mahan.[16] Using bulk parameters[17,18] for eq 1 results in $C_{el} = 82.8$ cm^{-1} nm for the diameter dependence of $\omega_{RBM} = C_{el}/d$.

In order to take into account also the microscopic structure of the CdSe nanostructures with and without a ZnS shell, we performed ab initio calculations. The geometries of the CdSe NWs were created on the basis of wurtzite-structured CdSe nanocrystals. The shell atoms Zn and S were initially placed on Cd and Se sites, respectively. Figure 1 displays exemplary cross sections of the relaxed NWs. The diameter of the NWs is defined by the average distance of the outermost atoms, including the ZnS shell, to the rotational axis.

We used the local density approximation[19] of the density functional theory with numerical atomic orbitals implemented in the SIESTA code.[20,21] The core electrons were replaced by pseudopotentials;[22] valence electrons were described by atom-centered confined numerical basis functions for the configurations Se:$4s^24p^4$, Cd:$5s^24d^{10}$, S:$3s^23p^4$, and Zn:$4s^23d^{10}$. We tested the convergence of the ab initio results with respect to the basis set completeness, the number of k-points and the real space mesh cutoff, for which a value of 140 Ry was used. A minimum number of four k-points were equally spaced along the one-dimensional Brillouin zone. The size of the basis, a double-ζ basis set plus an additional polarizing orbital, followed the standard split scheme and was controlled by an internal SIESTA parameter, the energy shift, for which a value of 50 meV was used. The structures were relaxed until all forces were below 0.02 eV/ and the stress along the axis was minimized with respect to the lattice constant. Although there is a strong lattice distortion after relaxation due to the lattice mismatch of the core−shell NWs, the 4-fold atomic coordination is explicitly retained for the structures calculated in this work. The force constants were obtained by finite differences, taking into account the symmetry of the wires.[23]

A detailed presentation of the vibrational properties, the influence of surface saturations on these properties, and the size dependence of the optical phonons will be published elsewhere.[24] The ab initio calculations reveal a vibrational mode where the atoms move almost radially, which is present in all calculated NWs. This mode is fully symmetric. An exemplary displacement pattern is displayed in Figure 2. The modes' frequency is diameter dependent, resulting frequencies of this RBM range from 40 to 160 cm^{-1} for a diameter range of 2.6−0.6 nm. As expected from eq 1, the calculated frequencies show a $1/d$ dependence on the diameter. The absolute values, however, are about 10 cm^{-1} larger than those predicted from elasticity theory and constitute a more precise estimate of the frequencies from a microscopic calculation.

To experimentally investigate the RBM in nanorods, CdSe nanorods of various sizes were grown by a standard technique based on the high temperature (300 °C) reaction between organometallic precursors of Cd (dimethylcadmium) and Se (trioctylphosphine selenide) in trioctylphosphine oxide in the presence of hexadecylphosphonic acid as a surface growth modifier.[2] An epitaxial ZnS shell, approximately two to three monolayers in thickness, was grown atop a selected nanorod sample in a second step in a hexadecylamine/trioctylphosphine oxide reaction mixture at (180 °C), with diethylzinc and thiourea as Zn and S precursors, respectively.[25]

For the Raman measurements the samples were placed on Si wafers and held in a commercial Oxford cryostat, which was evacuated to 2×10^{-6} mbar. The samples were cooled to liquid helium temperature. The 514 nm line of an Ar^+ laser was used as excitation source, the laser power was kept below 20 mW to avoid laser heating. The combination of a bandpass filter and a monochromator suppressed possible plasma lines. A Dilor-XY triple monochromator system in

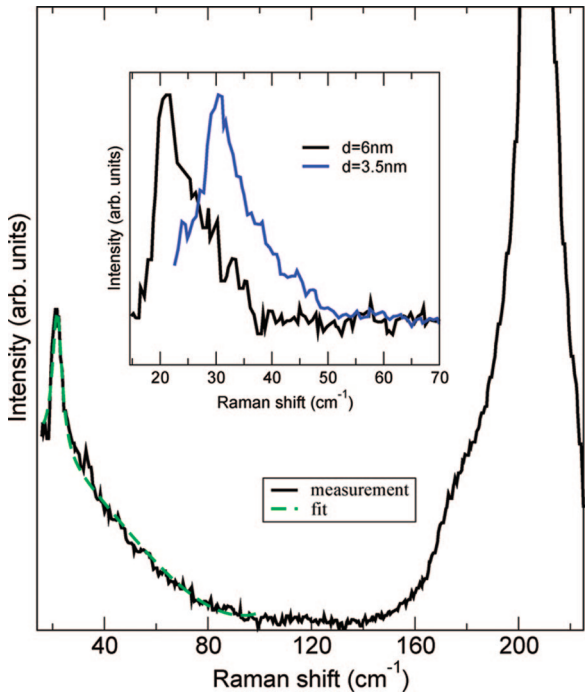

Figure 3. Raman spectrum from CdSe nanorods of 4 nm diameter and 25 nm length. Inset: low-frequency Raman spectra from nanorods of 3.5 nm diameter and 20 nm length and 6 nm diameter and 35 nm length. The laser-related background was subtracted.

backscattering geometry was used with a nitrogen-cooled CCD to acquire the Raman spectra. All samples were measured in two configurations, in focus and out of focus, to exclude possible artifacts due to, e.g., the presence of low-frequency rotational vibrations from ambient gases.

Figure 3 displays a Raman spectrum from CdSe nanorods of 4 nm diameter and 25 nm length in the low-frequency regime. The background present between 20 and 100 cm^{-1} is attributed to elastically scattered laser light and fitted with a cubic polynomial. Two Raman bands can be identified in the observed frequency range. The prominent asymmetric line around 200 cm^{-1} is attributed to the CdSe longitudinal optical phonon and has contributions from surface optical phonons.[26] The second observed band is located at lower frequencies and can be fitted with a Lorentzian function centered at 21.9 cm^{-1}.

To investigate the diameter dependence of the observed Raman band at low frequencies, we prepared samples of various sizes. Exemplary spectra are displayed in the inset of Figure 3. For nanorods with a diameter below 4 nm, the frequency of the band is shifted to higher frequencies, while it is shifted to lower frequencies for thicker nanorods. This behavior is as predicted for the RBM by eq 1 and our ab initio calculations. To exclude possible influences from the nanorod length and the aspect ratio on the position of the low-frequency Raman band, we took spectra from CdSe nanorods of the same diameter but different aspect ratio. No significant deviations of the modes frequency from nanorods 4 nm diameter and 30 nm length, compared to the frequency from the 4 × 25 nm^2 nanorods were found. The observed Raman band at low frequencies does only depend on the nanorod diameter, follows the diameter-dependent behavior

Table 1. Radial Breathing Mode Frequency of CdSe Nanorods

sample dimensions	ω_{RBM}, cm^{-1}
3.5 nm × 20 nm	29.8
4 nm × 25 nm	21.9
4 nm × 30 nm	21.7
6 nm × 35 nm	20.6

predicted for the RBM, and is thus assigned to the RBM. For nanorods with a diameter around 6 nm and above, the RBM is at quite low frequencies, which makes it harder to detect. We were not able to determine the position of the RBM from nanorods with diameters above 6 nm. Table 1 summarizes the observed RBM positions.

In order to obtain a value for the proportionality constant in $\omega_{RBM} \propto 1/d$, we fitted the calculated RBM frequencies and our experimentally obtained values. We weighted the individual data points according to their accuracy, taking into account the experimental and computational error, and fitted $\omega_{RBM} = C/d$ to the RBM frequency versus diameter data. The fit to the complete set of frequencies resulted in $\omega_{RBM} = 91.0\ cm^{-1}\ nm/d$. This yields an excellent agreement with the experimental diameter dependence of the RBM frequency. Figure 4 displays the measured and calculated RBM frequencies along with the C/d dependence. The determination of the RBM frequency allows a good approximation of the nanorod diameter with a macroscopic technique. The peak full width at half-maximum may be used as indicator for diameter distributions.

Included in the figure are calculated frequencies for CdSe NWs covered with a one- or two-monolayer ZnS shell. The RBM frequencies of the core−shell structures are higher by 7−15 cm^{-1} than their counterparts of bare CdSe. This is due to compressive strain and the shortened bonding lengths in the CdSe core with addition of the shell.[27] The effect increases with a thicker shell, and thin NWs are influenced more. To verify this observation experimentally, we measured the RBM of a CdSe nanorod with a diameter of 2.8 nm and a length of 22 nm, covered with a two to three monolayer ZnS shell. The RBM is at 52 cm^{-1}, 20 cm^{-1} higher than that expected for a bare nanorod of this diameter. The increase of the RBM frequency is somewhat larger but

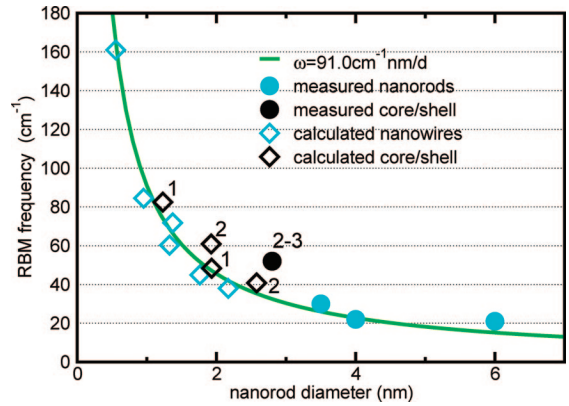

Figure 4. RBM frequency vs nanorod diameter. The curve results from a fit to the core structures only. The core−shell structures are labeled by the number of monolayers.

of the same magnitude as for the calculated NWs. This is due to the thicker shell of the measured nanorods compared to the shells of the calculated NWs, for which our calculational capacities were limited.

The measurement of the RBM is especially useful to determine the diameter of very thin nanorods where transmission electron microscopy is close to the resolution limit. The RBM frequency is very sensitive to diameter fluctuations below 4 nm, while the frequency of the RBM is less sensitive for diameter changes of thicker nanorods and vanishes for larger structures.

In conclusion we have directly observed the RBM in Raman spectra from CdSe nanorods. We demonstrated its purely radial dependence and estimated the diameter dependence of the RBM frequency from the experimental results and ab initio calculations of CdSe nanowires. Our results can be used to characterize thin nanorods via Raman spectroscopy. The RBM is shifted to higher frequencies when adding a ZnS shell to the nanorods. For related material systems like ZnO, ZnS, and ZnSe, where even smaller structures with diameters down to 1 nm exist,[28,29] we predict the existence of the RBM with similar dependences.

Acknowledgment. We acknowledge the Deutsche Forschungsgemeinschaft for financial support within the SPP 1165 framework.

References

(1) Alivisatos, A. *Science* **1996**, *271*, 933.
(2) Peng, X.; Manna, L.; Yang, W.; Wickham, J.; Scher, E.; Kadavanich, A.; Alivisatos, A. *Nature* **2000**, *404*, 59.
(3) Manna, L.; Scher, E.; Alivisatos, A. *J. Am. Chem. Soc.* **2000**, *122*, 12700.
(4) Thoma, S.; Sanchez, A.; Provencio, P.; Abrams, B.; Wilcoxon, J. *J. Am. Chem. Soc.* **2005**, *127*, 7611.
(5) Tavenner-Kruger, S.; Park, Y.; Lonergan, M.; Woggon, U.; Wang, H. *Nano Lett.* **2006**, *6*, 2154.
(6) Gerion, D.; Pinaud, F.; Williams, S.; Parak, W.; Zanchet, D.; Weiss, S.; Alivisatos, A. *J. Phys. Chem. B* **2001**, *105*, 8861.
(7) Aharoni, A.; Oron, D.; Banin, U.; Rabani, E.; Jortner, J. *Phys. Rev. Lett.* **2008**, *100*, 057404.
(8) Chilla, G.; Kipp, T.; Menke, T.; Heitmann, D.; Nikolic, M.; Froemsdorf, A.; Kornowski, A.; Foerster, S.; Weller, H. *Phys. Rev. Lett.* **2008**, *100*, 057403.
(9) Lange, H.; Artemyev, M.; Woggon, U.; Niermann, T.; Thomsen, C. *Phys. Rev. B* **2008**, *77*, 193393.
(10) Li, L.; Walda, J.; Manna, L.; Alivisatos, A. *Nano Lett.* **2002**, *3*, 961.
(11) Huynh, W.; Dittmer, J.; Alivisatos, A. *Science* **2002**, *259*, 2425.
(12) Alvarez, L.; Righi, A.; Guillard, T.; Rols, S.; Anglaret, E.; Laplaze, D.; Sauvajol, J. *Chem. Phys. Lett.* **2000**, *316*, 186.
(13) Jorio, A.; Pimenta, M.; Souza, A.; Saito, R.; Dresselhaus, G.; Dresselhaus, M. *New J. Phys.* **2003**, *5*, 139.
(14) Maultzsch, J.; Telg, H.; Reich, S.; Thomsen, C. *Phys. Rev. B* **2005**, *72*, 205438.
(15) Hu, M.; Wang, X.; Hartland, G. V.; Mulvaney, P.; Juste, J. P.; Sader, J. E. Vibrational Response of Nanorods to Ultrafast Laser Induced Heating: Theoretical and Experimental Analysis. *J. Am. Chem. Soc.* **2003**, *125*, 14925.
(16) Thonhauser, T.; Mahan, G. *Phys. Rev. B* **2005**, *71*, 081307.
(17) Cline, C. F.; Dunegan, H. L.; Henderson, G. W. Elastic Constants of Hexagonal BeO, ZnS, and CdSe. *J. Appl. Phys.* **1967**, *38*, 1944.
(18) Börnstein, L. *Group III Condensed Matter*; Volume 41: Semiconductors, II-VI and I-VII Compounds, Semimagnetic Compounds; Springer: Heidelberg.
(19) Perdew, J. P.; Zunger, A. Self-interaction correction to density-functional approximations for many-electron systems. *Phys. Rev. B* **1981**, *23*, 5048.
(20) Ordejón, P.; Artacho, E.; Soler, J. M. Self-consistent order-*N* density-functional calculations for very large systems. *Phys. Rev. B* **1996**, *53*, R10–441.
(21) Soler, J. M.; Artacho, E.; Gale, J. D.; García, A.; Junquera, J.; Ordejon, P.; Sanchez-Portal, D. The SIESTA method for ab initio order-*N* materials simulation. *Phys. Condens. Matter.* **2002**, *14*, 2745.
(22) Troullier, N.; Martins, J. L. Efficient pseudopotentials for plane-wave calculations. *Phys. Rev. B* **1991**, *43*, 1993.
(23) Yin, M. T.; Cohen, M. L. *Phys. Rev. B* **1982**, *26*, 3259.
(24) Mohr, M.; Thomsen, C. (arXiv:0802.3975v2).
(25) Manna, L.; Scher, E.; Li, L.; Alivisatos, A. *J. Am. Chem. Soc.* **2002**, *124*, 7136.
(26) Lange, H.; Machón, M.; Artemyev, M.; Woggon, U.; Thomsen, C. *Phys. Status Solidi RRL* **2007**, *1*, 274.
(27) Mohr, M.; Thomsen, C. *Phys. Status Solidi B* **2008**, *245*, 2111.
(28) Panda, A.; Acharya, S.; Efrima, A. *Adv. Mater.* **2005**, *17*, 2471.
(29) Pradhan, N.; Efrima, S. *J. Phys. Chem. B* **2004**, *108*, 11964.

NL803134T